Solar-Terrestrial Physics. 2024. Vol. 10. Iss. 3. P. 91–96. DOI: 10.12737/stp-103202411. © 2024 G.A. Makarov. Published by INFRA-M Academic Publishing House

UDC 550.385.4
DOI: 10.12737/stp-103202411

Received March 05, 2024
Accepted April 08, 2024

LARGE-SCALE RELATIONSHIPS OF THE GEOMAGNETIC INDICES *SYM-H* AND *ASY-H* WITH THE NORTH-SOUTH IMF COMPONENT AND THE SOLAR WIND BETA PARAMETER

G.A. Makarov
Yu.G. Shafer Institute of Cosmophysical Research and Aeronomy SB RAS,
Yakutsk, Russia, gmakarov@ikfia.ysn.ru

Abstract. Using annual average values, the relationships are examined of the geomagnetic indices *SYM-H*, *ASY-H*, and *Dst* with solar wind parameters in 1981–2015. The data used was divided into two samples according to the sign of the north-south component B_n of the interplanetary magnetic field (IMF). Variations in the annual average values of each of the *Dst*, *SYM-H*, and *ASY-H* indices for southward and northward IMF have been found to be similar and their linear correlation coefficients *r* to be high: 0.871, 0.863, and 0.943 respectively. The similarity between variations of the indices with different signs of B_n is probably due to their connection with the number of sunspots. It has been established that *Dst*, *SYM-H*, and *ASY-H* depend on the solar wind parameter β: their absolute values decrease with increasing β, regardless of B_n sign. The decrease in the indices with increasing β is likely to be caused by the transition of the magnetosphere to a quiet state due to the increasing predominance of thermal pressure over magnetic one in the solar wind and a decrease in the level of solar wind turbulence. *SYM-H* and *ASY-H* have been found to reveal the closest relationships with β, whereas *SYM-H* more strongly depends on β for southward IMF (r=0.744) than for northward IMF (r=0.677). On the contrary, for *ASY-H* r=–0.741 at northward IMF and r=–0.719 at southward IMF. Similar to *SYM-H*, *Dst* (to a lesser extent) significantly correlates with β at southward IMF (r=0.629) and weaker at northward IMF (r=0.456).

Keywords: geomagnetic indices *Dst*, *SYM-H*, and *ASY-H*, geomagnetic activity, magnetospheric ring current, interplanetary parameters.

INTRODUCTION

The geomagnetic indices *Dst*, *SYM-H*, and *ASY-H* are used to characterize the magnetospheric ring current: *Dst* measures its intensity [Sugiura, Kamei, 1991], *SYM-H* and *ASY-H* distinguish symmetric and asymmetric components [Iyemori et al., 1992]. The method of determining *Dst* is detailed in [Sugiura, Kamei, 1991]; *SYM-H* and *ASY-H*, on [http://wdc.kugi.kyoto-u.ac.jp/aeasy/asy.pdf]. It is significant that *SYM-H* is, in fact, averaged deviations of the geomagnetic field components *H* and *D* from the quiet level at observation stations corrected for geomagnetic latitude, whereas *ASY-H* is defined as a range between maximum and minimum values of the *H* and *D* components after subtracting the corresponding symmetric parts from the disturbance field. *SYM-H* generally has negative values, as *Dst* does, whereas *ASY-H* is always positive.

The contributions of the ring current, magnetopause and magnetotail currents, as well as field-aligned currents, to *Dst*, *SYM-H*, and *ASY-H* have been determined to date [Alexeev et al., 1996; Maltsev et al., 1996; Greenspan, Hamilton, 2000; Kalegaev et al., 2005; Dubyagin et al., 2014; Tsyganenko, Sitnov, 2005].

Geomagnetic activity is well known to depend strongly on solar wind (SW) velocity, modulus, southward and azimuthal components, as well as variability of the interplanetary magnetic field (IMF). The interplanetary electric field, the SW electromagnetic energy flux, as well as various combinations of interplanetary medium parameters are considered as geoeffective characteristics. How the interplanetary parameters affect geomagnetic activity is thoroughly reviewed, for example, in [Newell et al., 2007; Liemohn et al., 2018, Lockwood, McWilliams, 2021].

The relationship between *SYM-H*, *SYM-D*, *ASY-H*, *ASY-D* and the interplanetary parameters is examined in [Weygand, McPherron, 2006; http://wdc.kugi .kyoto-u.ac.jp/aeasy/asy.pdf] from one-minute data; the authors have found offsets in the indices. According to the definition given in these papers, the offset is a non-zero index value under magnetically quiet conditions. The offsets were assumed to be the total contribution of the ring current and the magnetopause and magnetotail current systems existing in the magnetosphere during magnetically quiet periods. In [Makarov, 2021], offsets in *SYM-H* and *ASY-H* have been estimated for *Dst*≥0 and when considering their regression relations with *Dst*.

Singh et al. [2013] have studied the effect of smoothly and sharply changing conditions of the IMF north-south component on the low-latitude indices *ASY-H* and *ASY-D* during magnetic substorms. Shi et al. [2006] have found that with a negative IMF north-south component an increase in the SW dynamic pressure further increases the ring current asymmetry. The results also show that mid-latitude disturbances of the geomagnetic field horizontal component around the local noon or midnight, as well as *ASY-H*, often exhibit a significant contribution of field-aligned currents. Haiducek et al. [2017] have employed the SWMF system to model the prediction of the geomagnetic indices K_p, *SYM-H*, *AL* and have found that the model excels at predicting *SYM-H* with a standard error 17–18 nT. Bhaskar and Vichare [2019] have used an artificial neural network to successfully predict *SYM-H* and *ASY-H* during nine geomagnetic storms of solar cycle 24. The SW velocity and density, as well as IMF, were utilized as input data. During the main phase of strong storms there are noticeable deviations indicating the influence of internal factors such as magnetospheric processes. In [Makarov, 2022], the dependences of *SYM-H* and *ASY-H* on key interplanetary parameters have been examined using extensive statistical data and it has been established that the contribution of the IMF modulus should be taken into account when describing the relationship of *ASY-H* and *SYM-H* with the IMF north-south component.

Many studies have dealt with variations in geomagnetic disturbances and interplanetary parameters in the solar cycle. The main patterns of such changes are well-known (see, e.g., [Obridko et al., 2013; Richardson et al., 2000; Yermolaev et al., 2018]). Kurazhkovskaya [2020] has drawn attention to the role of the SW β parameter in developing a geomagnetic storm. The β parameter is a ratio of the SW thermal pressure to the magnetic one $\beta=((4.16\ T/10^5)+5.34)N/B^2$, where T is the temperature, N is the proton density, B is the IMF modulus. Kurazhkovskaya et al. [2021] have found a nonlinear relationship between *Dst* and average β during magnetic storms. Yermolaev et al. [2009] have proposed to use β for identifying SW streams of different types.

In this paper, the dependence of *SYM-H*, *ASY-H*, and *Dst* on the IMF north-south component and the β parameter is examined using annual averages.

EXPERIMENTAL DATA IN USE

The variations in annual average *Dst*, *SYM-H*, and *ASY-H* and interplanetary parameters from 1981 to 2015 are investigated. The data for 1989 is excluded from consideration due to the lack of information about auroral indices the relationship with which is still to be analyzed. Information on the indices is taken from the website of the World Data Center for Geomagnetism [https://wdc.kugi.kyoto-u.ac.jp/index.html]; and on the solar wind and the sunspot number, from NASA's Space Physics Data Center [http://omniweb.gsfc.nasa.gov/]. The IMF components in this database are represented in the RTN coordinate system: the R-axis is directed radially from the Sun; the T-axis, toward the solar rotation; and the N-axis is the cross product of the R- and T-axes. At zero heliographic latitude, the N-axis and the axis of solar rotation are parallel. The RTN and GSE coordinate systems at near-Earth distances differ in the opposite directions of the R- and X-axes, as well as T- and Y-axes, respectively.

RESULTS AND DISCUSSION

Figure 1 illustrates variations in the annual average geomagnetic indices *Dst*, *SYM-H*, and *ASY-H* (*a*) for the IMF north-south component B_n of opposite signs: $B_n\leq0$ and $B_n>0$, as well as the ratio between the indices (*b*) for $B_n\leq0$ and $B_n>0$. At $B_n\leq0$, the absolute values of all three indices are seen to be noticeably higher than at $B_n>0$ throughout the period.

This higher geoeffectiveness of IMF with $B_n\leq0$ is well-known (e.g., [Bazarzhapov et al., 1979]). The above mentioned pattern is clearly seen in plots of the ratios: the ratio is higher than 1; at $B_n\leq0$, *Dst*, *SYM-H*, and *ASY-H* are, on average, 1.8, 1.7, and 1.2 times higher than at $B_n>0$ respectively. The sharp increase in the *Dst* ratio (top right panel) is due to the minimum absolute value of this index in 2009 at $B_n>0$.

Comparison between variations of each index for $B_n\leq0$ and $B_n>0$ in Figure 1 shows that they are similar and their correlation coefficients are high: for *Dst*, *SYM-H*, and *ASY-H*, r=0.871±0.028, 0.863±0.029, and 0.943±0.013 respectively. For IMF B_n of different signs, IMF annual average B varies similarly, r=0.973; for the IMF north-south component B_n, r=–0.863 (Figure 2, *a* and *b* respectively), as well as for other key SW parameters: velocity, proton density and temperature r=0.946, 0.931, and 0.924 respectively. The interplanetary parameters are known to depend on solar activity level [Kovalenko, 1983]. The similarity between the index variations at B_n of different signs can be assumed to be due to their relationship with the sunspot number.

Comparison between annual variations in the geomagnetic indices (see Figure 1, *a*) and the sunspot number R_i (see Figure 2, *d*) shows that *Dst*, *SYM-H*, and *ASY-H* vary relative to R_i in the same way, i.e. their strongest perturbations are observed during solar maximum.

Cross-correlation analysis to identify shifts between time series of the geomagnetic indices without dividing data by the sign of IMF B_n relative to the sunspot number R_i has revealed that all three indices and R_i vary nearly synchronously. So, when the *Dst* series is shifted by 1 year to the left relative to the R_i series, r=–0.638±0.069; without a shift, r=–0.637±0.068; by 1 year to the right, r=–0.380±0.100; by 2 years to the right, r=–0.122±0.117. When the *SYM-H* series shifts, we have the following r: –0.762±0.049, –0.762±0.048, –0.520±0.085, and –0.224±0.112 respectively. The shift in the *ASY-H* series yields 0.642±0.069, 0.703±0.058, 0.576±0.078, and 0.322±0.106 respectively.

Previously, the relationship between *Dst* and solar activity has been examined in detail in [Echer et al., 2011; Yermolaev et al., 2013] when studying the development of geomagnetic storms. Echer et al. [2011] have found that geomagnetic storms have a two-peak distribution: one peak is close to the solar maximum, the other is at the beginning of the descending phase. Yermolaev et al. [2013] indicate that the occurrence of magnetic storms is determined by interplanetary structures of different types. Correlation plots of the geomagnetic indices and sunspot number are presented in Figure 3.

Figure 2, along with variations in annual average IMF B (*a*), IMF north-south component B_n (*c*), and sunspot number R_i (*d*), illustrates variations in the β parameter (*b*) characterizing the ratio between thermal and magnetic energies in SW. The B variations for B_n of opposite signs can be seen to be almost identical, the coefficient of their mutual correlation r=0.973; variations in β (r=0.946) also coincide; B_n varies in antiphase (r=–0.863).

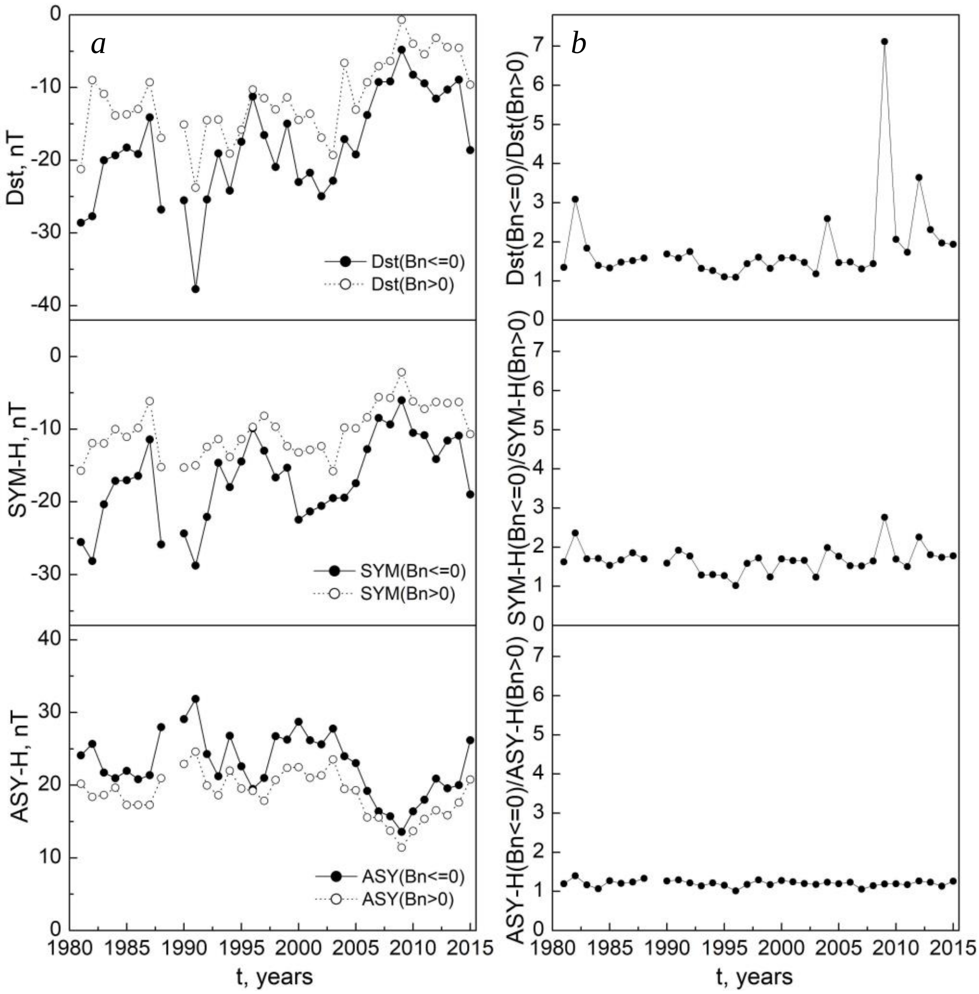

Figure 1. Variations in the annual average geomagnetic indices *Dst, SYM-H,* and *ASY-H* in 1981–2015 for IMF B_n of opposite signs: $B_n \leq 0$ (solid lines), $B_n > 0$ (dotted lines) (*a*); ratios between the indices for $B_n \leq 0$ and $B_n > 0$ (*b*)

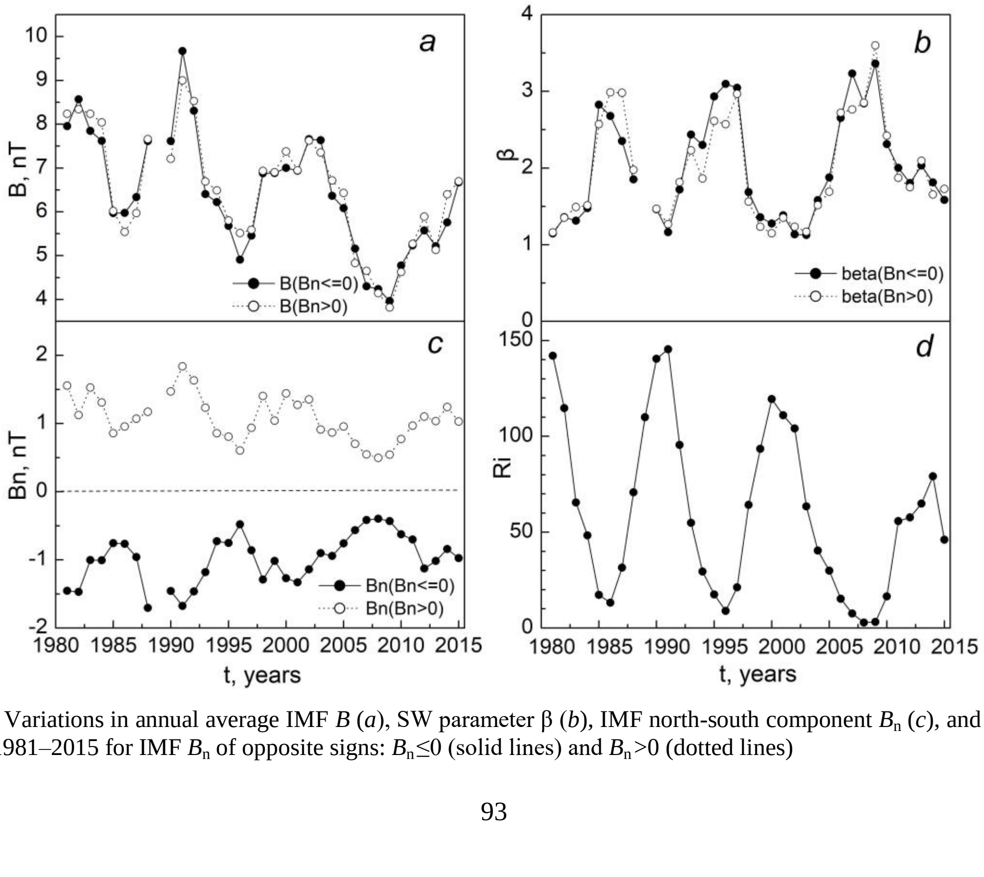

Figure 2. Variations in annual average IMF *B* (*a*), SW parameter β (*b*), IMF north-south component B_n (*c*), and sunspot number R_i (*d*) in 1981–2015 for IMF B_n of opposite signs: $B_n \leq 0$ (solid lines) and $B_n > 0$ (dotted lines)

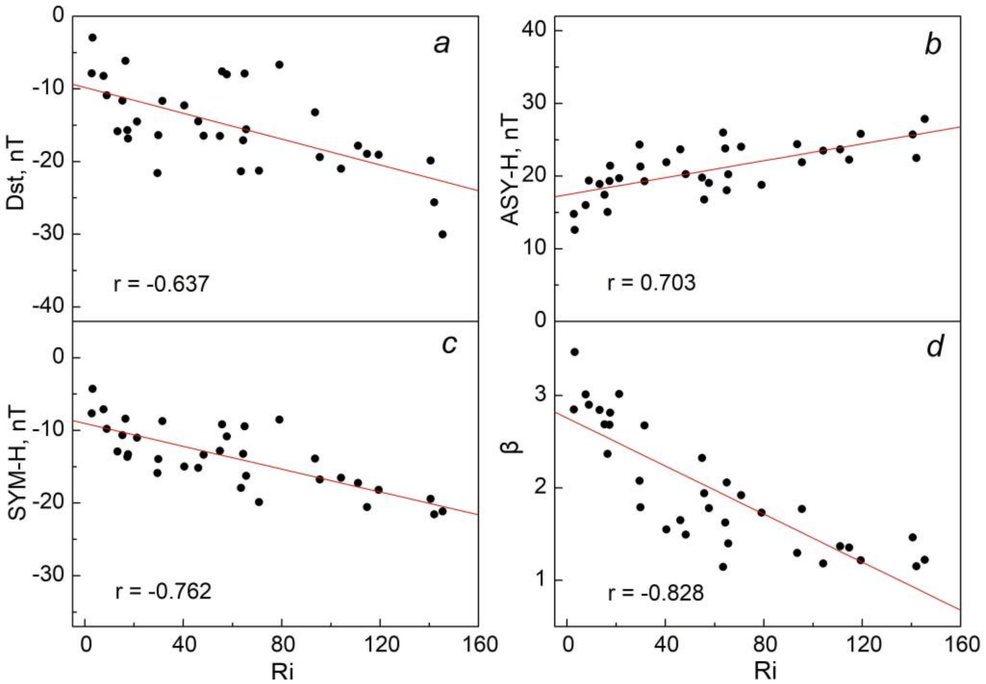

Figure 3. Variations in *Dst* (*a*), *ASY-H* (*b*), *SYM-H* (*c*), and β (*d*) relative to the sunspot number *Ri* regardless of the B_n sign; *r* represents linear correlation coefficients

All three parameters closely correlate with R_i. When comparing variations in *B* and R_i regardless of IMF direction, we get r=0.795; between β and R_i, r=–0.828, i.e. *B* and R_i vary synchronously; β and R_i vary in antiphase. Note that β>1, and this probably indicates an excess of thermal pressure over magnetic pressure with long-term averaging of the SW parameters. During high solar activity, *B* increases and, accordingly, β decreases. A decrease in β reflects an increase in magnetic pressure and hence maximum plasma turbulence. This regularity is described in [Kurazhkovskaya et al., 2021; Kurazhkovskaya, Kurazhkovsky, 2023]. Comparing B_n and R_i regardless of B_n sign shows there is no connection between them (r=–0.005). That is understandable because the south and north fields neutralize each other when summed up. If we examine them separately for southward and northward IMF, the relationship between B_n and R_i is fairly close: for B_n≤0, r=–0.864; for B_n>0, r=0.845.

Figure 3 illustrates the dependences of the geomagnetic indices (*a*–*c*) and the β parameter (*d*) on R_i, regardless of the B_n orientation. The corresponding regression equations are obtained: *Dst*=–0.089 R_i–9.786; *ASY-H*=0.058 R_i+17.462; *SYM-H*=–0.079 R_i–9.048; β=–0.013 R_i+2.755. It is clearly seen that as R_i increases the absolute values of the three indices increase, β decreases. The decrease in β reflects an increase in the SW magnetic pressure and hence an increase in geomagnetic activity.

Figure 4 illustrates the dependence of the indices on β at B_n of opposite signs and the correlation coefficients *r* between the indices and β. All three indices at southward IMF are seen to be much larger in value than at northward IMF, whereas absolute values of the indices decrease with increasing β regardless of the B_n sign. *SYM-H* and *ASY-H* exhibit the closest relationships with β, whereas *SYM-H* depends more strongly on β at B_n≤0 (r=0.744) than at B_n>0 (r=0.677). Conversely, *ASY-H* is more closely related to β at B_n>0 (r=–0.741) than at B_n≤0 (r=–0.719). Similarly, *SYM-H Dst* (to a lesser extent) appreciably correlates with β at B_n≤0 (r=0.629) and weaker at B_n>0 (r=0.456). The decrease in the indices in absolute value with increasing β is probably due to the increasing predominance of thermal pressure over magnetic pressure in SW.

Plots in Figure 4 can be approximated by linear functions; the regression equations are as follows:

- at B_n≤0, *Dst*=6.59β–31.45, *SYM-H*=6.29β–29.46, *ASY-H*=–4.44β+31.71;
- at B_n>0, *Dst*=3.69β–18.92, *SYM-H*=3.47β–17.14, *ASY-H*=–3.34β+25.45.

Regression coefficients in *SYM-H* and *Dst* equations at B_n≤0 are ~1.8 times higher than at B_n>0. This can be explained by the fact that the symmetric component of the ring current weakens more strongly at B_n≤0 than at B_n>0 during the transition of the magnetosphere from the disturbed state to a quieter one, i.e. with an increase in β. For *ASY-H*, the ratio between the coefficients differs 1.3 times and at B_n≤0, when the magnetosphere becomes quiet, the asymmetric component of the ring current also weakens faster than at B_n>0, but at a lower rate than the symmetric one. Similar ratios are obtained for absolute terms of the regression equations for the indices and β.

The dependence of *Dst* on β derived in this work is generally consistent with the result obtained in [Kurazhkovskaya et al., 2021], taking into account the fact that we operated on annual averages when the effects of storm phases and interplanetary fluxes of different types being summed up are leveled. In the cited work based on hourly average data, the similarity between the dynamics of *Dst* and β during geomagnetic storms with gradual and sudden onsets has been established and the relationship between *Dst* and β has been shown to be nonlinear.

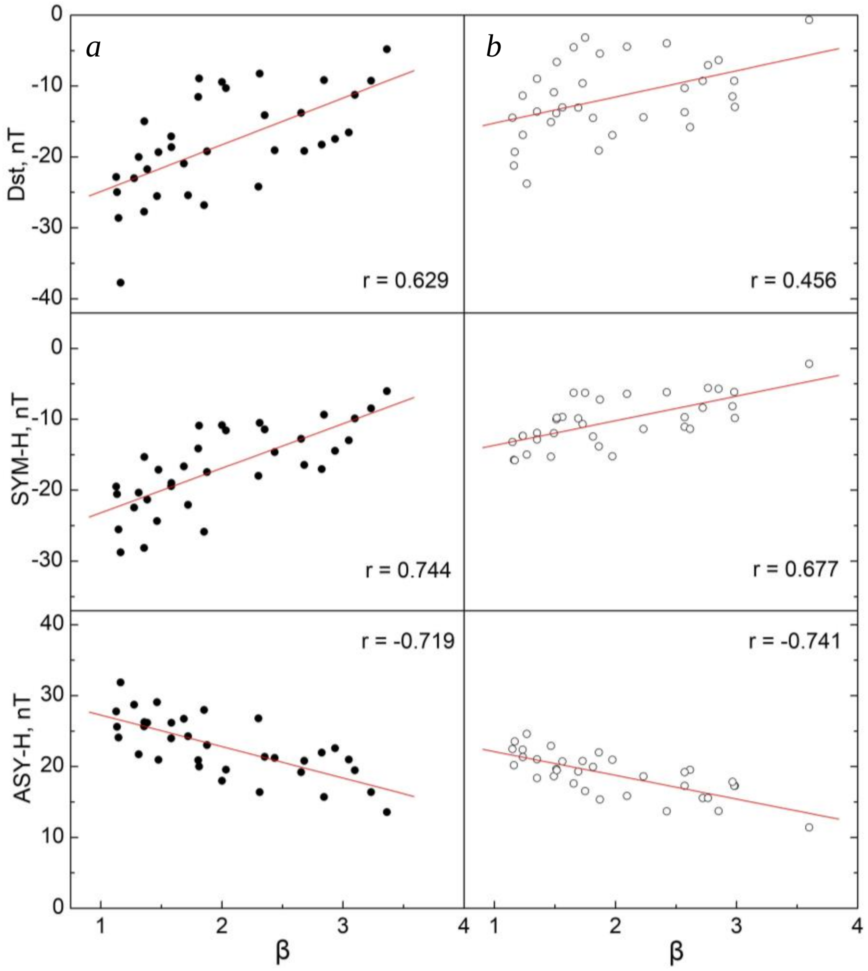

Figure 4. *Dst*, *SYM-H*, and *ASY-H* as function of β at B_n≤0 (*a*) and B_n>0 (*b*); *r* represents linear correlation coefficients

CONCLUSION

Study of the relationships of the geomagnetic indices *Dst*, *SYM-H*, and *ASY-H* according to their annual averages with SW parameters in 1981–2015 has shown that they are consistent with the known patterns.

- For southward IMF (B_n≤0), the annual average geomagnetic indices *Dst*, *SYM-H*, and *ASY-H* in absolute value are much higher than for northward IMF (B_n>0) throughout the period considered. This fact of higher IMF geoeffectiveness with B_n≤0 is well-known. It has been found that at B_n≤0 *Dst*, *SYM-H*, and *ASY-H* are, on average, 1.8, 1.7, and 1.2 times higher than at B_n>0 respectively.
- As expected, annual average *SYM-H*, as *Dst* does, varies relative to the sunspot number R_i in antiphase; and *ASY-H*, in phase: the indices are extreme in years of R_i maxima and minima.
- With increasing solar activity, the β parameter decreases, which means an increase in the SW magnetic pressure and hence in geomagnetic activity due to an increase in turbulence.

The following main results have been obtained.

- Variations in annual averages of each of the *Dst*, *SYM-H*, and *ASY-H* indices at southward and northward IMF are similar and their correlation coefficients are high: 0.871, 0.863, and 0.943 respectively. The similarity between the variations is probably due to their relationship with the sunspot number.
- It has been established that *SYM-H* and *ASY-H* depend on the SW parameter β and their absolute values decrease with increasing β regardless of the sign of the IMF north-south component. The decrease in the indices with increasing β is likely due to the transition of the magnetosphere to a quiet state in response to increasing predominance of thermal pressure over magnetic pressure in SW and decreasing turbulence.
- It has been found that *SYM-H* and *ASY-H* exhibit the closest relationships with β, whereas *SYM-H* depends more strongly on β at B_n≤0 (*r*=0.744) than at B_n>0 (*r*=0.677). Conversely, *ASY-H* is more closely related to β at B_n>0 (*r*=–0.741) than at B_n≤0 (*r*=–0.719). Similarly, *SYM-H Dst* (to a lesser extent) appreciably correlates with β at B_n≤0 (*r*=0.629) and weaker at B_n>0 (*r*=0.456).

I am grateful to the team of the World Data Center (Kyoto, Japan) for providing access to the data on the geomagnetic indices and to the team of NASA's Goddard Space Flight Center for the solar wind and solar activity data.

The work was carried out under Government assignment (State Registration Number 122011700182-1).

REFERENCES

Alexeev I.I., Belenkaya E.S., Kalegaev V.V., Feldstein Y.I., Grafe A. Magnetic storms and magnetotail currents. *J. Geophys. Res*. 1996, vol. 101, no. A4. P. 7737–7747. DOI: 10.1029/95JA03509.

Bazarzhapov A.D., Matveev M.I., Mishin V.M. Geomagnitnye variatsii i buri [Geomagnetic Variations and Storms]. Novosibirsk, Nauka Publ., 1979, 248 p. (In Russian).

Bhaskar A., Vichare G. Forecasting of SYMH and ASYH indices for geomagnetic storms of solar cycle 24 including St. Patrick's day, 2015 storm using NARX neural network. *J. Space Weather Space Climate*. 2019, vol. 9, A12. DOI: 10.1051/swsc/2019007.

Dubyagin S., Ganushkina N., Kubyshkina M., Liemohn M. Contribution from different current systems to SYM and ASY midlatitude indices. *J. Geophys. Res.: Space Phys*. 2014, vol. 119, pp. 7243–7263. DOI: 10.1002/2014JA020122.

Echer E., Gonzalez W.D., Tsurutani B.T. Statistical studies of geomagnetic storms with peak *Dst*≤–50 nT from 1957 to 2008. *J. Atmos. Solar-Terr. Phys*. 2011, vol. 73, pp. 1454–1459. DOI: 10.1016/j.jastp.2011.04.021.

Greenspan M.E., Hamilton D.C. A test of the Dessler-Parker-Sckopke relation during magnetic storms. *J. Geophys. Res*. 2000, vol. 105, no. A3, pp. 5419–5430.

Haiducek J.D., Welling D.T., Ganushkina N.Y., Morley S.K., Dogacan Su Ozturk. SWMF Global Magnetosphere Simulations of January 2005: Geomagnetic Indices and Cross-Polar Cap Potential. *Space Weather*. 2017, vol. 15, pp. 1567–1587.

Iyemori T., Araki T., Kamei T., Takeda M. Mid-latitude geomagnetic indices ASY and SYM (provisional). Data Anal. Cent. For Geomagn. and Space Magn., 1992. Faculty of Sci., Kyoto Univ., Kyoto, Japan.

Kalegaev V.V., Ganushkina N.Y., Pulkkinen T.I., Kubyshkina M.V., Singer H.J., Russell C.T. Relation between the ring current and the tail current during magnetic storms. *Ann. Geophys*. 2005, vol. 23, pp. 523–533. DOI: 10.5194/angeo-23-523-2005.

Kovalenko V.A. Solnechny veter [Solar wind]. Moscow, Nauka Publ, 1983. 272 p. (In Russian).

Kurazhkovskaya N.A. Global disturbance of Earth's magnetosphere and its connection with space weather. *Solar-Terr. Phys*. 2020, vol. 6, iss. 1, pp. 41–49. DOI: 10.12737/stp-61202005.

Kurazhkovskaya N.A., Kurazhkovskii A.Yu. Hysteresis effect between geomagnetic activity indices (A_p, *Dst*) and interplanetary medium parameters in solar activity cycles 21–24. *Solar-Terr. Phys*. 2023, vol. 9, iss. 3, pp. 68–76. DOI: 10.12737/stp-93202308.

Kurazhkovskaya N.A., Zotov O.D., Klain B.I. Relationship between geomagnetic storm development and the solar wind parameter β. *Solar-Terr. Phys*. 2021, vol. 7, iss. 4, pp. 24–32. DOI: 10.12737/stp-74202104.

Liemohn M.W., McCollough J.P., Jordanova V.K., Ngwira C.M., Morley S.K., Cid C., et al. Model evaluation guidelines for geomagnetic index predictions. *Space Weather*. 2018, vol. 16, pp. 2079–2102. DOI: 10.1029/ 2018SW002067.

Lockwood M., McWilliams K.A. On optimum solar wind magnetosphere coupling functions for transpolar voltage and planetary geomagnetic activity. *J. Geophys. Res*. 2021, vol. 126, e2021JA029946. DOI: 10.1029/2021JA029946.

Makarov G.A. Offsets in the geomagnetic indices of the magnetospheric ring current. *Solar-Terr. Phys*. 2021, vol. 7, iss. 3, pp. 29–35. DOI: 10.12737/stp-73202103.

Makarov G.A. Geomagnetic indices ASY-H and SYM-H and their relation to interplanetary parameters. *Solar-Terr. Phys*. 2022, vol. 8, iss. 4, pp. 36–43. DOI: 10.12737/stp-84202203.

Maltsev Y.P., Arykov A.A., Belova E.G., Gvozdevsky B.B., Safargaleev V.V. Magnetic flux redistribution in the storm time magnetosphere. *J. Geophys. Res*. 1996, vol. 101, no. A4, pp. 7697–7704.

Newell P.T., Sotirelis T., Liou K., Meng C.-I., Rich F.J. A nearly universal solar wind-magnetosphere coupling function inferred from 10 magnetospheric state variables. *J. Geophys. Res.* 2007, vol. 112, A01206. DOI: 10.1029/2006JA012015.

Obridko V.N., Kanonidi Kh.D., Mitrofanova T.A., Shelting B.D. Solar Activity and Geomagnetic Disturbances. *Geomagnetism and Aeronomy*. 2013, vol. 53, no. 2, pp. 147–156. DOI: 10.1134/S0016793213010143.

Richardson I.G., Cliver E.W., Cane H.V. Sources of geomagnetic activity over the solar cycle: Relative importance of coronal mass ejections, high-speed streams, and slow solar wind. *J. Geophys. Res*. 2000, vol. 105, no. A8, pp. 18,203–18,213. DOI: 10.1029/1999JA000400.

Shi Y., Zesta E., Lyons L.R., Yumoto K., Kitamura K. Statistical study of effect of solar wind dynamic pressure enhancements on dawn-to-dusk ring current asymmetry. *J. Geophys. Res*. 2006, vol. 111, A10216. DOI: 10.1029/2005JA011532.

Singh A.K., Sinha A.K., Pathan B.M., Rajaram R., Rawat R. Effect of prompt penetration on the low latitude ASY indices. *J. Atmos. Solar-Terr. Phys*. 2013, vol. 94, pp. 34–40. DOI: 10.1016/j.jastp.2012.12.015.

Sugiura M., Kamei T. Equatorial *Dst* index 1957–1986. *IAGA Bull*. 1991, no 40, 14 p.

Tsyganenko N.A., Sitnov M.I. Modeling the dynamics of the inner magnetosphere during strong geomagnetic storms. *J. Geophys. Res*. 2005, vol. 110, A03208. DOI: 10.1029/2004JA010798.

Weygand J.M., McPherron R.L. Dependence of ring current asymmetry on storm phase. *J. Geophys. Res*. 2006, vol. 111, A11221. DOI: 10.1029/2006JA011808.

Yermolaev Yu.I., Nikolaeva N.S., Lodkina I.G., Yermolaev M.Yu. Catalog of Large-Scale Solar Wind Phenomena during 1976–2000. *Cosmic Res*. 2009, vol. 47, no. 2, pp. 81–94. DOI: 10.1134/S0010952509020014.

Yermolaev Y.I., Lodkina I.G., Nikolaeva N.S., Yermolaev M.Y. Occurrence rate of extreme magnetic storms. *J. Geophys. Res.: Space Phys*. 2013, vol. 118, pp. 4760–4765. DOI: 10.1002/jgra.50467.

Yermolaev Y.I., Lodkina I.G., Nikolaeva N.S., Yermolaev M.Y., Riazantseva M.O., Rakhmanova L.S. Statistic study of the geoeffectiveness of compression regions CIRs and Sheaths. *J. Atmos. Solar-Terr. Phys*. 2018, vol. 180, pp. 52–59. DOI: 10.1016/j.jastp.2018.01.027.

URL: http://wdc.kugi.kyoto-u.ac.jp/aeasy/asy.pdf (accessed October 5, 2021).

URL: https://wdc.kugi.kyoto-u.ac.jp/index.html (accessed March 29, 2023).

URLhttp://omniweb.gsfc.nasa.gov/ (accessed March 29, 2023).

This paper is based on material presented at the 19th Annual Conference on Plasma Physics in Solar System, February 5–9, 2024, IKI RAS, Moscow.

Original Russian version: Makarov G.A., published in Solnechno-zemnaya fizika. 2024. Vol. 10. No. 3. P. 97–103. DOI: 10.12737/szf-103202411. © 2024 INFRA-M Academic Publishing House (Nauchno-Izdatelskii Tsentr INFRA-M)

How to cite this article

Makarov G.A. Large-scale relationships of the geomagnetic indices *SYM-H* and *ASY-H* with the north-south IMF component and the solar wind beta parameter. *Solar-Terrestrial Physics*. 2024. Vol. 10. Iss. 3. P. 91–96. DOI: 10.12737/stp-103202411.